Libertas Academica
FREEDOM TO RESEARCH

ORIGINAL RESEARCH

X-ray Shielding Ability and Electrophysical Characteristics of Rubber Vulcanizates: Effect of State-of-Mix

M. Madani[1] and A.I. Abd-El Hafez[2]

[1]Radiation Physics Dept., National Center for Radiation Research and Technology (NCRRT), Cairo, Egypt. [2]Radiation Metrology Dept., National Institute for Standards (NIS), Giza, Egypt.

Abstract: Rubber composite materials were prepared using styrene-butadiene-rubber as matrices and incorporating with carbon black and PbO_2 for X-ray shielding. The pure gum SBR was firstly masticated with different mastication times before mixing. It was found that the mastication time strongly affected the microstructure of the prepared composites and in turn, the degree of cross-link density. The mastication time greatly improves the dispersion level of the used fillers. The effect of mastication time on the conductivity, current-voltage characteristics and TSDC of composites was investigated. The X-ray shielding ability of all composites apparently increases with the increase in mastication time. X-ray shielding ability of the prepared composites was also studied at different applied voltage and current of X-ray machine.

Keywords: rubber, X-ray, shielding, processing parameters, electric field, PTC, TSDC

This article is available from http://www.la-press.com.

Introduction

X-ray and gamma ray sources are presently being used in a wide array of medical and industrial machinery, and the breadth of such use expands from year to year. Consumers tend to notice medical and dental X-ray machines, but in addition to these applications there are baggage screening machines, non-destructive industrial inspection machinery and ion implantation machines used in the manufacture of silicon wafer computer chips. Medical equipment and devices that produce X-rays and gamma rays must be shielded to protect operators, clinicians, patients and sensitive electronic components from tube leakage and room scatter.

Lead is the most common shielding material used to protect against X-rays and γ-rays. However, the presence of a rapidly changing magnetic field, which induces eddy current in a conductor, makes the use of ordinary metallic lead un-acceptable.[1] Therefore, lead-polymer composites are used to make electrical insulator items. Lead has been used as a solid casting, as a solid encased within a polymer matrix, or as filler. As filler, it may be lead particles, tribasic lead-sulfate or lead-oxide particles or particles of a specified shape or size, or as a mixture with other materials such as tin. Tungsten shielding, or polymer-tungsten shielding has also been used.[2–4]

Ion implantation machine source insulators, X-ray tube insulation, radioisotope housings, other castings and housings could benefit from the properties of polymer-metal composite materials. In the case of typical high voltage insulators for ion implantation machinery, a thick walled generally round or cylindrical part is created out of lead or polymer-lead-oxide ranging from several centimeters to several decimeters in long dimension and weighing anywhere up to 200 kg. Wall thickness may range from 1 cm to several inches. Such parts must resist high voltages, shield against X-ray or gamma ray emission and hold a high vacuum state when connected to the vacuum chamber. High voltage X-ray shielding for X-ray tube insulators is generally thinner (often 0.15 cm thickness), generally smaller, and of different shape, having an aperture for the X-ray beam, but once again must offer high voltage insulation and radiation protection.

DC resistivity of an insulating material at a given temperature is a technologically important parameter. Many of the electrical designs require the knowledge of temperature dependence of resistivity.[5] Furthermore, the resistivity of polymeric insulating materials such as ethylene propylene rubber EPR, ethylene propylene diene rubber EPDM and styrene butadiene rubber SBR is in general varies with electrical field (also called electrical stress in electrical engineering). Measurements of temperature and electrical field dependences of resistivity of such rubber provide not only the value of resistivity but also its temperature and field coefficients, which are essential to many high voltage electrical applications. Introducing conductive Pb particles would in general reduce the resistivity of rubber. However, these particles may also create electron traps that would lead to a decrease in charge carrier mobility and hence increase the resistivity. Using thermally stimulated discharge current (TSDC) technique, the influence of chemical impurities that lead to the capture of charge carriers in electron traps can be studied with high sensitivity.[6] TSDC method also provides information on the mechanism of electrical conductivity of polymers; it can also lead to a better understanding of the long-lived electrostatic charging of polymeric materials, which is due to the charge storage in electron traps.

In this paper we study the effect of state of mix on the X-ray shielding ability and electrical properties of PbO$_2$ loaded SBR composites. The temperature and electrical field dependences of DC conductivity, and the thermally stimulated discharge current were also studied.

Experimental
Materials
Styrene-butadiene rubber (SBR, 1502), ISAF N220 carbon black, cure activators (zinc oxide and stearic acid) and curatives system based on sulphur were supplied by Transport and Engineering Co. (TRENCO), Alex., Egypt. The basic characteristics of SBR and ISAF are given in Table 1. The lead oxide PbO$_2$ (AR 239.21) was obtained from The Brurish Drug Houses (BDH Laboratory Chem. Ltd.), Poole, England.

Designation of filled SBR
SBR masterbatch was designated as St$_{x/y}$, where S and t represent SBR and mastication time respectively, and the suffixes x and y represent carbon black and PbO$_2$ loading, respectively. The sample designations are

Table 1. Rubber and carbon black characteristics.

Materials	Parameter	
Styrene-butadiene rubber (SBR-1502)	Styrene content (%)	23.5
	Volatile matter (%)	0.75
	Organic acid	4.75
	Ash	1.50
	Antioxidant	0.50
	Density (g/cc)	0.94
	Mooney viscosity (ML_{1+4}; 100 °C)	46.0
Carbon black ISAf (N220)	mean particle size (nm)	20
	pour density (gcm^{-3})	0.35
	DBP[a] adsorption (cc/100 g)	115
	CTAB[b] surface area (m^2/g)	115
	Ash (% Max.)	1.0

[a]Dibutyl phthalate.
[b]Cetyl trimethyl ammonium bromide.

tabulated in Table 2. The gradient are presented in parts per hundred part from rubber by weight (phr).

Mastication, compounding and vulcanization

The experiment was commenced by masticating SBR on a laboratory two-roll mill for various times (5, 10 and 15 min) at 75 °C.[7,8] in order to studying the effect of mastication time on the average molecular weight of rubber. Hence, the increase in mixing temperature acts favorably for the carbon-black-formed homogenous distribution through the SBR matrix.[7,8] Then the zinc oxide (ZnO) and stearic acid were added. The mixing was continued further for 2 min and then the carbon black and processing oil was charged and batches were produced with mixing times of 2 min. PbO$_2$ then subsequently added and mixed for 2 min. The curatives system, Dibenthiazyl disulfide (MBTS), tetramethyl thiuram disulphide (TMTD) and sulphur were, subsequently, added and mixed for 2 min before discharge and, finally, sheeted on a cooled two-roll mill. The rubber compound was then compression-moulded for 30 min under a pressure of 40 kg/cm^2 by using a hot-platen hydraulic in order to give vulcanized rubber using a cure temperature of 150 °C. The details of the compounding procedure were carried out as in previous work.[9]

Determination of average molecular weight

The average molecular weight $\bar{M}_c$ of the rubber vulcanizates from all systems were determined using Flory–Rehner equation [(Eq. (1))], the detail of the test procedure being found in previous work.[10]

$$\bar{M}_c = -V_1 \rho_p \frac{(V_m^{1/3} - V_m^{1/2})}{\ln(1 - V_m) + V_m + \chi_1 V_m^2} \qquad (1)$$

Table 2. Compound formulation details.

Ingredients (phr)	Mastication time								
	5	10	15	5	10	15	5	10	15
	S5$_{0/0}$	S10$_{0/0}$	S15$_{0/0}$	S5$_{40/0}$	S10$_{40/0}$	S15$_{40/0}$	S5$_{40/100}$	S10$_{40/100}$	S15$_{40/100}$
SBR	100	100	100	100	100	100	100	100	100
Stearic acid	2	2	2	2	2	2	2	2	2
ZnO	5	5	5	5	5	5	5	5	5
Oil	10	10	10	10	10	10	10	10	10
ISAF				40	40	40	40	40	40
PbO$_2$							100	100	100
MBTS	2	2	2	2	2	2	2	2	2
TMTD	1	1	1	1	1	1	1	1	1
S	2.5	2.5	2.5	2.5	2.5	2.5	2.5	2.5	2.5

where V_1 is the molar volume of the solvent (benzene = 89 cc/mol), ρ_p is the polymer density, V_m is the polymer volume fraction, and χ_1 is the Flory-Huggins interaction parameter between solvent and rubber (0.362 in this work).

For all samples, swelling data were used to calculate $V_m = 1/Q_m$,[10] where Q_m is the equilibrium degree of swelling of the composites in a given sample swollen to equilibrium in solvent and given by[11]

$$Q_m = (1 + \frac{\rho_p\,(Q_w - 1)}{\rho_s})$$ (2)

where Q_w is the ratio of the weights of the network in the swollen and dry state, and ρ_s is the density of the solvent. Three samples per formulation were tested.

Sample irradiation

The cross-linked materials were used in the form of specimens with dimensions $150 \times 150 \times 2$ mm and were subjected to ^{60}Co γ-irradiation at a dose rate 7.75 kGy/h at 40 °C. The ^{60}Co γ-source model GB150 type B manufactured by the AEA of Canada and located at NCRRT, Egypt.

Measurements of electrical properties

The electrical measurements were carried out using a programmable DC voltage/current generator, along with a precision digital electrometer (Keithley) to determine the current generated on application of a known voltage to filled rubber vulcanisates having containing the percolation dose (40 phr) of conducting carbon black filler.[10] For measuring the temperature dependence of the resistivity, the sample was enclosed in a temperature-controlled thermostat, and temperature was altered at a rate of 0.5 °C/min (the rate was kept the same for the measurements during the heating and cooling cycle). The measurement procedure has been described elsewhere.[12]

Thermally stimulated polarization and depolarization

Thermally stimulated polarization was conducted at a specific polarization temperature, $T_p = 120$ °C under the application of 3 kV/cm electrical field. The voltage was applied for 2 h and the sample was then cooled at 0.5 °C/min to 25 °C, at which time the voltage was turned off and the sample was shorted to remove frictional and stray charges.[6] After 10 minutes, the depolarization currents were measured during a 0.5 °C/min temperature ramp to about 100 °C. The measurement procedure has been described elsewhere.[6]

Shielding performance

The X-ray machine in this work is MCN 323 metal-ceramic Philips double pole X-ray tube. The MG325 Philips X-ray system is highly stabilized constant potential X-ray system with a Tungsten anode material and 4 mm inherent Beryllium filter. The H.V. and tube current adjustment range are from 15–320 kV and from 0 to 22.5 mA respectively.

The measurements were performed in the Secondary Standard Dosimetry Laboratory (SSDL) in the national Institute for Standards (NIS) using calibrated UNI-DOS electrometer type 10001 with cylindrical ionization chamber manufactured by PTW-FREIBURG, Germany. It is a universal dosimeter for simultaneous dose and dose rate measurements in radiotherapy, diagnostic radiology and health physics. It fulfills all requirements on dosimeters of the reference class according to IEC 731.[13] The dosimetry system has been caliprated in the Bureau International Des Poids Et Measures (BIPM) France.

X-ray shielding ability of the prepared composites was studied at different applied voltage (70 and 100 kV) and different current (5, 10 and 15 mA) of X-ray machine.

In order to determine the value of lead-equivalence (LE) for the given rubbers, it was necessary to make a curve of Pb standard sheets with a series of thickness as a function of their attenuation coefficients. Through the interpolation of attenuation coefficients of the measured rubber in the curve, the value of LE can be determined and expressed accordingly in mm Pb.

Results and Discussion

In order to obtain a composite matrix possibly showing clear electrophysical characteristics, it has been found that the carbon black CB and PbO_2 fillers must be appropriately well dispersed inside the composite matrix through a suitable mixing process. Accordingly, in following sections, main attentions will be focused on how to prepare a desired composite material which possesses a highly cross-linked network

structure and shows an acceptable X-ray shielding ability via state of mix (mastication time, MT).

Effect of mastication time on the degree of cross-linking

One of the basic parameters that describe the structure of polymer network is the molecular weight between cross-links of swollen network. This describes the molecular weight of polymer chains between two consecutive junctions. These junctions may be chemical cross-links, physical entanglements, crystalline regions or even polymer complexes.[10] The Flory–Rehner theory is used to determine $\bar{M}_c$ and average cross-linking densities of polymer networks (v_e). v_e, which is defined as the number of elastically effective chains, totally included in a perfect network, per unit volume,[14] can be calculated from;[10]

$$v_e = \frac{\rho_p N}{\bar{M}_c} \qquad (3)$$

where N is Avogadro's number.

The influences of mastication time on v_e and $\bar{M}_c$ of the un-filled and filled vulcanizates are listed in Table 3. $\bar{M}_c$ of SBR compounds were reduced by increasing the mastication time. The decrease in $\bar{M}_c$ of the matrix with increasing MT is accompanied by increase in v_e as expected. For un-filled vulcanizates the cross-link density is found to be less affected than the filled one with increase in MT.[15] Higher cross-link density is observed for 40 phr CB loaded SBR samples and as

MT increases v_e also increases. This is attributed to the filler-filler and filler-polymer network formations. The stronger the rubber-filler network, the higher the reinforcement. Thus, a stronger interaction between CB and polymer is required for better reinforcement of polymer matrix by the filler, which leads to the increase in v_e of CB filled matrix. Meanwhile, v_e of the CB/SBR composites were reduced by addition of 100 phr of PbO_2, this is due to the non-reinforcing nature of PbO_2.

The improvement of network properties with mastication time might be related to reduction of the molar mass of the rubber matrix as MT increase,[16] which enhances the effective dispersion of filler in SBR matrix. Moreover, as the mixing temperature increased (75 °C) and the molar mass decreased, the viscosity of the matrix phase was decreased, which in turn facilitated the breakup process of the filler agglomerates, and resulting in relatively high dispersion of the filler and further improvement of the rubber properties will achieved.[7]

Effect of γ-irradiation on the degree of cross-linking

The above mentioned samples were exposed to γ-irradiation in air with different doses (50, 100, 200 and 500 kGy) to studying its radiation stability. The variation of $\bar{M}_c$ and v_e data of all rubber vulcanizates with γ-irradiation dose are presented in Table 3. It is observed that v_e values increases and $\bar{M}_c$ decreases with irradiation dose. The increase in v_e with radiation

Table 3. The average molecular weight and the average cross-link density of all compositions.

Dose, kGy →	$\bar{M}_c$ (m gm/ mol)					$v_e *10^{-18}$ (m^{-3})				
Sample	0	50	100	200	500	0	50	100	200	500
S5$_{0/0}$	2.55	2.45	3.36	2.31	2.31	2.01	2.09	1.52	2.22	2.22
S10$_{0/0}$	2.43	2.40	2.41	2.41	2.35	2.11	2.13	2.12	2.12	2.18
S15$_{0/0}$	2.22	2.21	2.21	2.15	2.11	2.31	2.32	2.32	2.38	2.43
S5$_{40/0}$	1.27	1.22	1.21	1.12	1.12	545.11	567.45	572.14	618.12	618.12
S10$_{40/0}$	1.13	1.12	1.06	1.05	0.96	612.65	618.12	653.11	659.33	721.14
S15$_{40/0}$	0.74	0.72	0.71	0.69	0.65	935.54	961.52	975.07	1003.3	1065.07
S5$_{40/100}$	1.97	1.85	1.82	1.72	1.62	427.81	455.56	463.07	490.0	520.24
S10$_{40/100}$	1.96	1.91	1.85	1.81	1.61	430.0	441.25	455.56	465.63	523.47
S15$_{40/100}$	1.32	1.22	1.24	1.15	1.05	638.4	690.8	679.6	732.86	802.6

dose is evidence of formation of a three-dimensional network structure. The results strongly suggest that radiation exposure in air causes more cross-linking that increases the value of v_e. Moreover, it is interesting to note that the un-filled samples are marginally affected by the irradiation dose. This is because SBR matrix has excellent resistance to radiation.[17] Furthermore, at higher radiation doses; there is a possibility of chain scission. From the present data, it is apparent that network formation dominates over the scission of the network. Also, if scission predominates at higher doses, the increase in the number of network chains per unit volume can be accounted for by the fact that chain fractures might lead to entanglements, which then act as cross-links.[18]

Effect of mastication time on the electrical properties
Current-voltage (I–V) characteristics

Although carbon black dominates the conductive electrical properties of filled rubber,[19] the main purpose of using carbon black in this research is to reinforce the rubber compounds and to achieve antistatic protection.[19]

The current-voltage I–V characteristics of unfilled ($S15_{0/0}$ only for comparison) and all filled vulcanizates were studied at 25 °C and 90 °C. I–V characteristics of CB filled vulcanizates at 25 °C are shown in Figure 1 in the form of plots of log current density and electric field. The current density J flowing through a specimen across which an electric field E is applied at certain temperature is given by[20]

$$J = J_0 \sinh\left(\frac{aeE}{2KT}\right) \qquad (4)$$

where a, is the jump distance of charge carrier, T is the temperature in Kelvin, e is the electron charge, K is Boltzmann's constant, and J_0 is a fitting parameter that depends on the operating condition of the polymer. Figure 2 shows how well the results, for $S5_{40/0}$ sample as an example, fit this formula over a wide range of the field. The parameters a and J_0 were detected for all studied compositions and presented in Table 4. The parameters a and J_0 were found to be strongly dependent upon the changes in the network structure of the fillers that induced by different MT. The jumping distance in rubber compounds depends
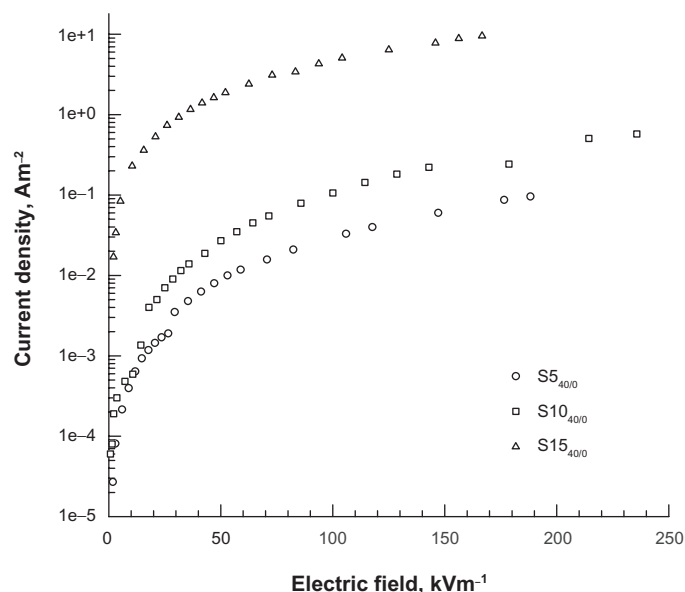

Figure 1. Plot of log (current density) vs. electric field at room temperature for CB/SBR composites.

on filler type and size,[21] cross-link density[22] and homogeneous dispersion of compound ingredients.[23] Higher MT showed a lower a (higher J), proving the higher filler distribution in the matrix. The composites containing CB and PbO_2 showed a higher jumping distance than that containing CB only.

As a conclusion, higher MT could, therefore, lead to the following results: 1 smaller size of carbon
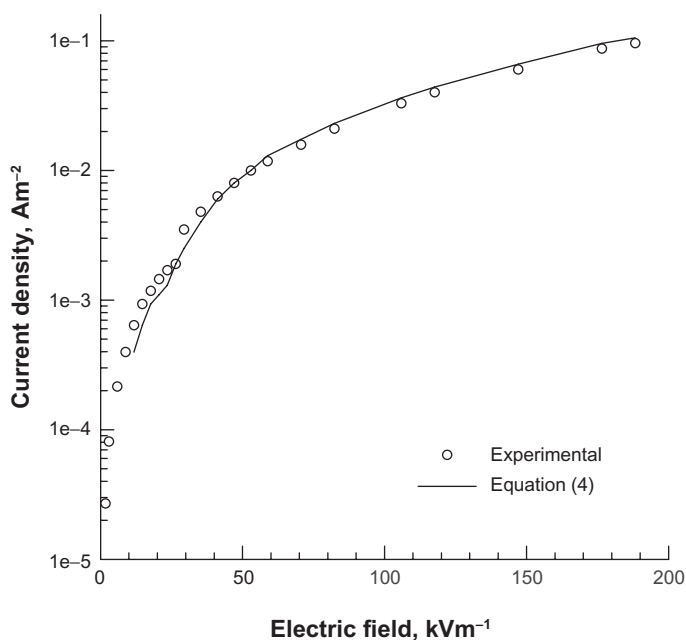

Figure 2. Log current density for $S5_{40/0}$ versus electric field at room temperature: experimental data and fitting using Eq. (4).

Table 4. The fitting parameters data (α and J_0) and electrical field coefficient of conductivity (β) for different compounds.

Sample	α (μm)	J_0 (Am⁻²)	β (m/kV)	α (μm)	J_0 (Am⁻²)	β (m/ kV)
	at 25 °C			**at 90 °C**		
S15$_{0/0}$	215	66.2×10^{-11}		218	36.5×10^{-10}	
S5$_{40/0}$	96	36.4×10^{-6}	3.0	101	24.3×10^{-6}	3.0
S10$_{40/0}$	91	66.2×10^{-7}	2.75	99	35.1×10^{-6}	4.03
S15$_{40/0}$	72	41.2×10^{-8}	1.71	76	68.5×10^{-7}	1.0
S5$_{40/100}$	102	69.4×10^{-8}	8.39	104	63.7×10^{-8}	1.72
S10$_{40/100}$	99	54.2×10^{-8}	1.4	102	17.3×10^{-8}	2.09
S15$_{40/100}$	85	63.5×10^{-7}	2.99	76	36.0×10^{-8}	1.2

black aggregates which are in favor of enhancing the formation of higher conductive networks compared with the composites with the same filler content;[24] 2) higher dispersion of carbon black, lowering inter-particle-distance from one another and consequently increasing the conductivity of the matrix.[24] The conductivity of composite material is the competitive result of these effects. It seems that, these two effects dominate the conductivity of the composite, that is, in respect to the same CB content, when a higher MT is applied; the conductivity of composite concomitantly increases as shown later.

The conductivity and its electrical field coefficient

The DC current has been measured as a function of the DC voltage applied to all composites at 30 and 90 °C. Although Ohm's Law does not generally hold for dielectrics at high electrical fields, one can still define resistance as $R = V/I$. It then follows that the conductivity σ of polymer matrix is given by

$$\sigma = \frac{I \cdot d}{A \cdot V} = \frac{J}{E} \tag{5}$$

where d is the sample thickness, A is the electrode cross section area. The log conductivity of all composites has been plotted against mean DC electrical field >40 kV/m at selected temperature for CB loaded SBR (Figs. 3 and 4) and for PbO$_2$ and CB loaded SBR (Figs. 5 and 6). It can be seen that the conductivity is electrical field dependent. For all samples, the log conductivity increase approximately linearly with applied E. The electrical field dependence of conductivity can be described by the following equation[25]

$$\sigma = \sigma_0 \exp(-\beta E) \tag{6}$$

where β is the electrical field coefficient of conductivity and σ_0 is constant corresponding to σ at very small E. By fitting a straight line to the log conductivity versus electrical field data, β can be obtained from the gradient. The results of all composites are given in Table 4.

At higher MT (15 min.), β has a very small value (Table 4), indicating that DC conductivity of these composites is not sensitive to electrical field. At lower MT (5 min.), however, larger values of electrical field coefficient are obtained for the two samples studied. This observation may have important technical implications.
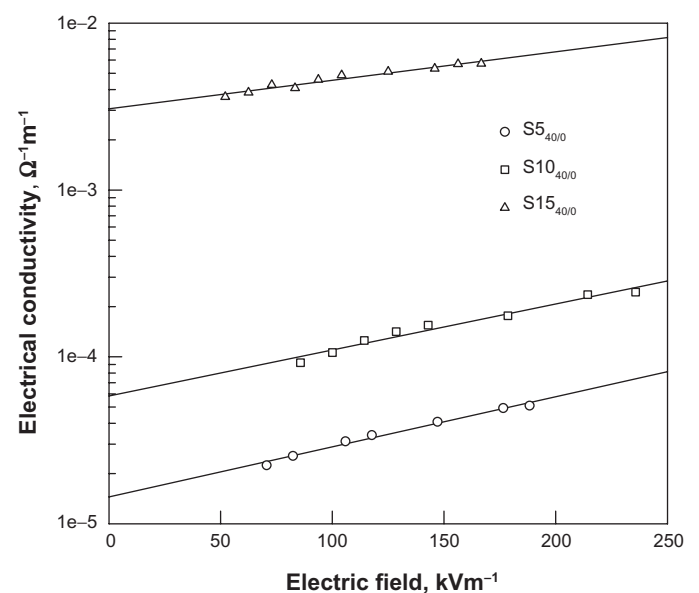
Figure 3. Electrical field dependence of DC conductivity of CB/SBR composites at 30 °C.
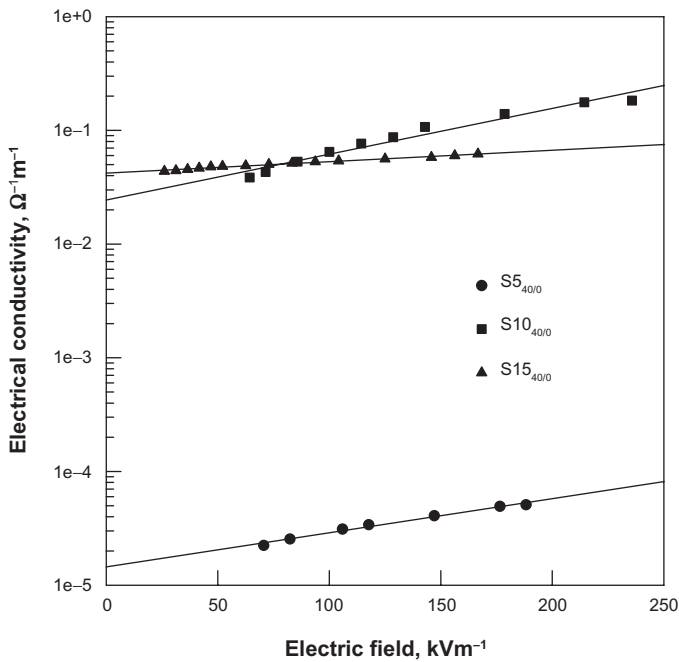
Figure 4. Electrical field dependence of DC conductivity of CB/SBR composites at 90 °C.

Since the change in electrical field coefficient due to an increase in MT may affect the electrical field distribution across the composite materials.

Effect of temperature on the electrical conductivity

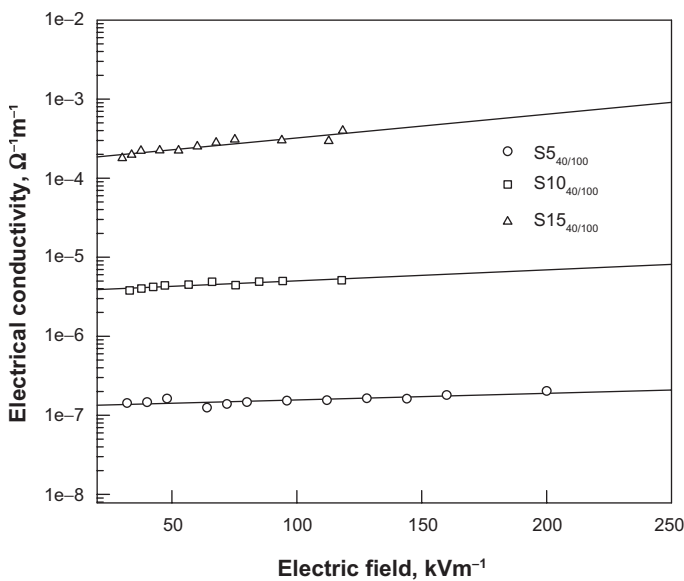In Figures 3–6 the results also indicate that σ of SBR composites is temperature dependent and this

Figure 5. Electrical field dependence of DC conductivity of PbO$_2$ filled CB/SBR composites at 30 °C.
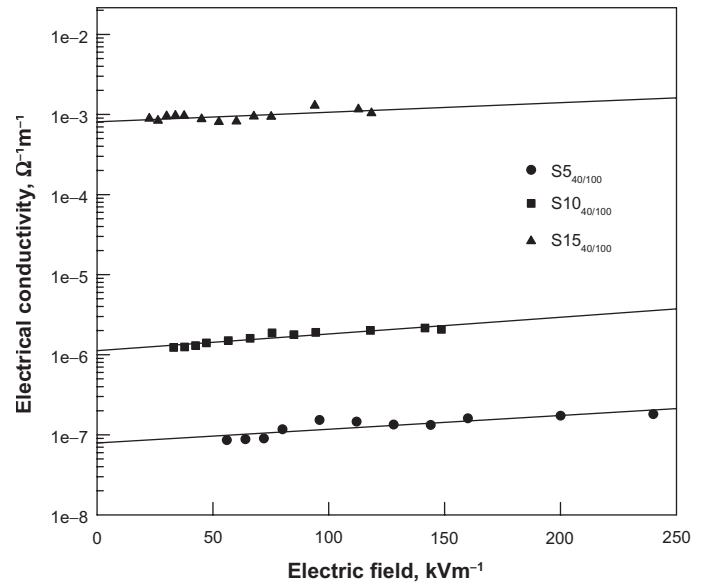
Figure 6. Electrical field dependence of DC conductivity of PbO$_2$ filled CB/SBR composites at 90 °C.

temperature dependence varies with electrical field. Electrical conductivity at a constant electrical field ≈ 7.5 kV/m versus temperature, T, for all samples loaded with 40 phr of ISAF CB are shown in Figure 7, while σ for those samples loaded with CB and PbO$_2$ are shown in Figure 8. Different behavior at different MT were observed for the variation of σ with temperature at the same filler content. The variation of σ with T was markedly dependent on MT. The dependency of σ on temperature for conductive polymer composites CPC is quite a complex phenomenon. The temperature
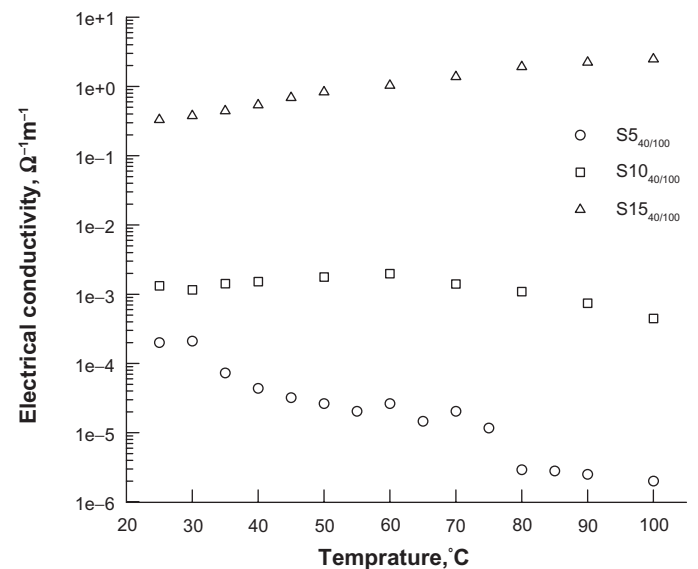

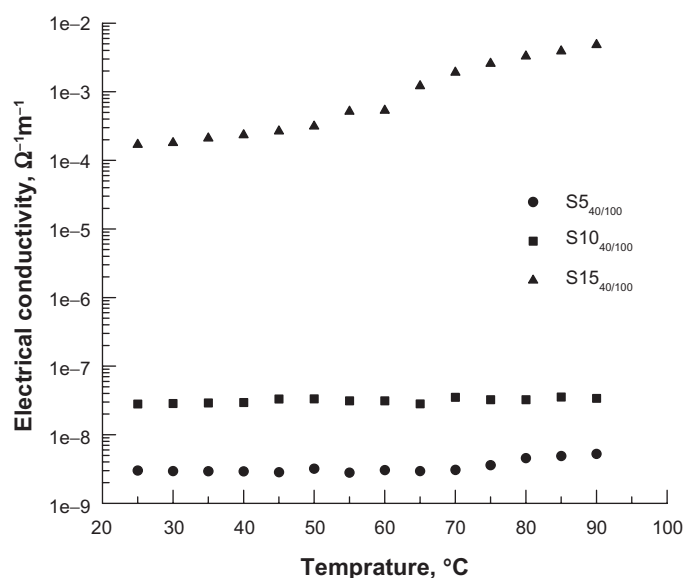**Figure 7.** Temperature dependence of DC conductivity for CB/SBR composites.

Figure 8. Temperature dependence of DC conductivity for PbO$_2$ filled CB/SBR composites.

coefficient of resistance may be positive (PCT), negative (NCT), or zero, depending on the type, nature and concentration of filler, the nature of the polymer matrix and the filler distribution.[26] The resistivity of carbon black–filled composite progressively increases with the increase in temperature at lower MT [i.e. a positive coefficient of temperature (PCT effect) was observed]. While, it decrease with the increase in temperature at higher MT [i.e. a negative coefficient of temperature (NCT effect) was observed]. These different behaviors can be explained based on conductive network stability and filler rearrangement. The appreciable PCT effect can be explained by the predominant breakdown of the conducting network structure attributed to differential thermal expansion of rubber matrix compared to the CB filler.[27] Because of an increased gap between conducting elements with the increase in temperature the resistivity increases (σ decrease); also the probability of electron hop or tunneling is reduced in this condition. On the other hand, the increase in the degree of cross-linking due to the increase in MT help SBR molecules to held together strongly through chemical interaction, which will more reduce the free volume inside the matrix and in turn, attenuate the breakdown of the conducting network structure. Moreover, the conductivity here is presumably sensitive to temperature because it is just at the percolation limit. Even small changes in the network structure would have the greatest effect on conductivity in the percolation region.

In comparison with Figure 7, the incorporation of PbO$_2$, in Figure 8, just imparts a less influence of temperature on the shape of curves of conductivity. The slopes of all the curves are almost constant and similar to each other except that, for the S15$_{40/100}$ sample, the conductivity is thermally activated. From Figures 7 and 8 it also can be seen that σ of all CB/SBR composites decreased due to the incorporation of 100 phr from PbO$_2$. As mentioned above lead oxide particles may also create electron traps that would lead to a decrease in charge carrier mobility and hence increase the resistivity.

Thermally stimulated depolarization current (TSDC)

In the electric field induced polarization under the action of heat (poling), permanent and induced dipoles orient either individually or under the influence of the motion of neighbouring groups. Thermal motion of the molecules continuously disrupts the orientation of the dipoles in the direction of the applied electric field so that a dynamic equilibrium ensues. Under the influence of the electrical field, charge carriers can also be injected into the sample.[25] These charges migrate to the oppositely charged electrodes and space charge can be built up in their vicinity. In general, TSDC gives information on dipole relaxation, charge injection and detraping processes in electrical insulation materials.[28] After poling (stressing) at the highest voltage and temperature, all the dipoles are lined up with the electrical field and their contribution to the DC current tends to be zero. The current measured now includes only the contribution from charge carriers, whether they are injected or activated from traps. Therefore, the temperature dependence of DC current under constant voltage will lead to a determination of trap depth.

According to theory, the space charge limited current density J that flows for an applied voltage V can be given by the Mott and Gurney square law[25]

$$J = \frac{9\varepsilon_0 \varepsilon_r V^2}{8 d^2} \cdot \theta \qquad (7)$$

where

$$\theta = \frac{n_c}{n_t} = \frac{N_{eff}}{N_t} \exp\left(-\frac{\Delta E_t}{kT}\right) \qquad (8)$$

is the ratio of free charge carriers to those trapped. In Equation (8), n_c and n_t are the densities of free charge carriers and trapped carriers respectively, N_t is the number density of traps with trap depth $-\Delta E_t$ (an energy below the bottom of the conduction band) and N_{eff} the effective density of states for the conduction band. Now, if Equation (8) was correct, an ln (DC current) versus $1/T$ plot would result in a straight line, which is exactly what we can see in Figure 9 for BC filled vulcanizates and Figure 10 for PbO_2 and BC filled vulcanizates. From the gradient of the straight line, the trap depth $-\Delta E_t$ has been calculated for all filled vulcanizates. The results are given in Table 5. Note that the band gap for EPR is 8.8 eV and we would assume a similar value for SBR formulation.[25] Note that the experimental data in Figures 9 and 10 have been obtained under constant voltage "after poling" and therefore is a direct consequence of long-range migration of charge carriers. This is rather different from the data given in Figures 7 and 8, which include contributions from both charge carriers and dipole reorientation. It is evident from Figures 9 and 10 that DC current increase as MT increases for all filled vulcanizates. However, PbO_2 particles may also result in an increase in the number of traps that would subsequently decrease the conductivity of CB/SBR composites. Moreover, as mentioned above, PbO_2 particles could reduce the mobility of the molecular dipoles, which will also lead to an increase in resistivity.

After the sample temperature reached the room temperature, the applied DC voltage was turned off and the sample was short circuited and discharged and then TSDC was measured. The TSDC spectra of the CB filled SBR and CB+PbO_2 filled SBR are given in Figures 11 and 12 respectively. The spectrum of CB filled vulcanizates (Fig. 11) consists of
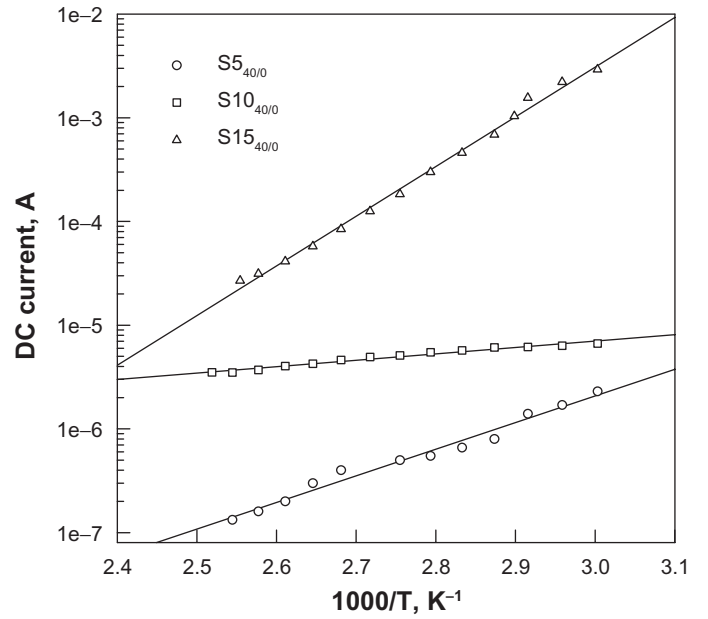

Figure 9. Temperature dependence of DC current for CB/SBR composites at a constant electrical field of 3 kV/cm. The data were obtained when the samples were cooled down to room temperature after poling.

mainly a broad positive peak (i.e. the current flow is in the normal discharge direction).[25] The peak height and peak temperature are decreased as MT increased as presented in Table 5. Although the discharge current includes contributions from both charge carriers
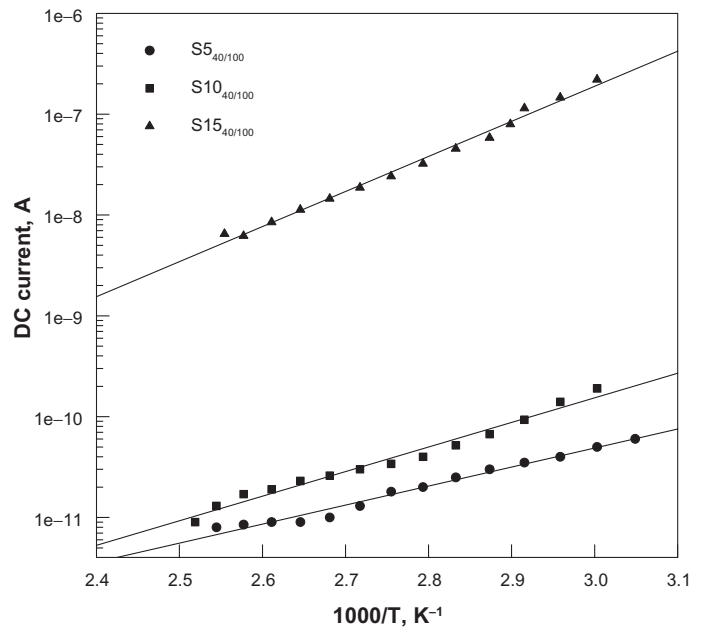
Table 5. TSDC peak position T_p, peak height I_p and trap depth ΔE for all filled vulcanizates with different MT.

Sample	T_p (°C)	I_p (pA)	ΔE (eV)
S5$_{40/0}$	102	88.6	0.21
S10$_{40/0}$	70	34	0.051
S15$_{40/0}$	55	8.7	0.41
S5$_{40/100}$	55	2.7	0.16
S10$_{40/100}$	60	9.9	0.2
S15$_{40/100}$	65	5200	0.31

Figure 10. Temperature dependence of DC current for PbO_2 filled CB/SBR vulcanizates at a constant electrical field of 3 kV/cm. The data were obtained when the samples were cooled down to room temperature after poling.
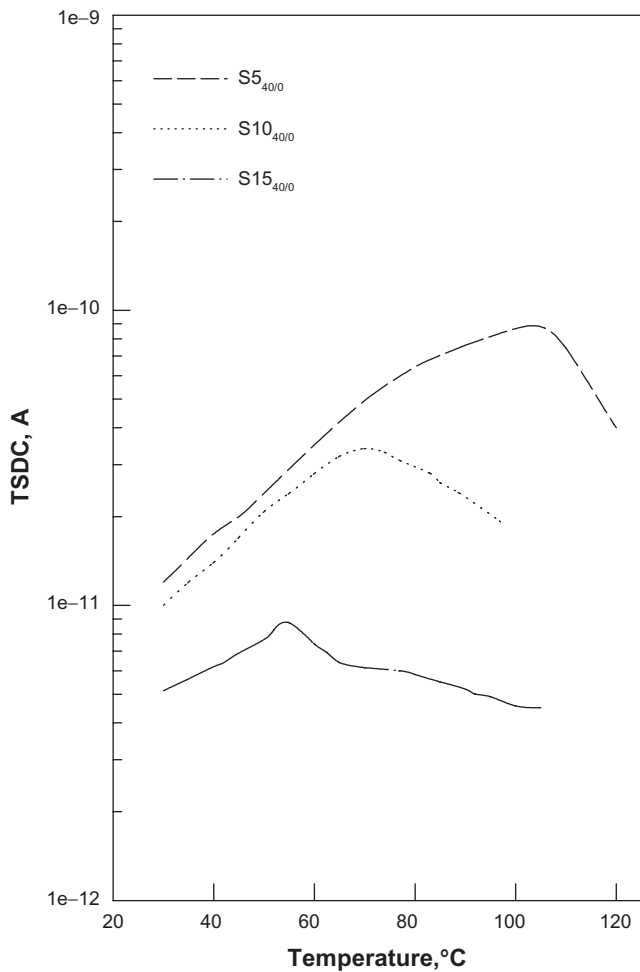
Figure 11. Temperature dependence of TSDC current for CB/SBR vulcanizates with different MT.

Figure 12. Temperature dependence of TSDC current for PbO_2 filled CB/SBR vulcanizates with different MT.

and dipoles, the main feature of the spectrum arises from orientational relaxation of the dipoles within the insulation. TSDC peak height is a measure of the density of trapped carriers and frozen dipoles in the poled material. It can be seen from Figure 11 that the peak height for sample $S15_{40/0}$ with higher MT is the lowest. This means that fewer charges were trapped and fewer dipoles were frozen in the sample during the poling. In any case, the releasing of charges, whether they are trapped carriers or frozen dipoles, seems to be dominantly controlled by the molecular motion in the polymer. TSDC peak temperature T_p is directly related to the electron trap depth: while charge carriers in shallow traps can be released at low temperatures, higher temperature is needed to activate the charges in deep traps. The broad TSDC peak observed for the three samples indicates that there is a distribution in the trap depth.[25]
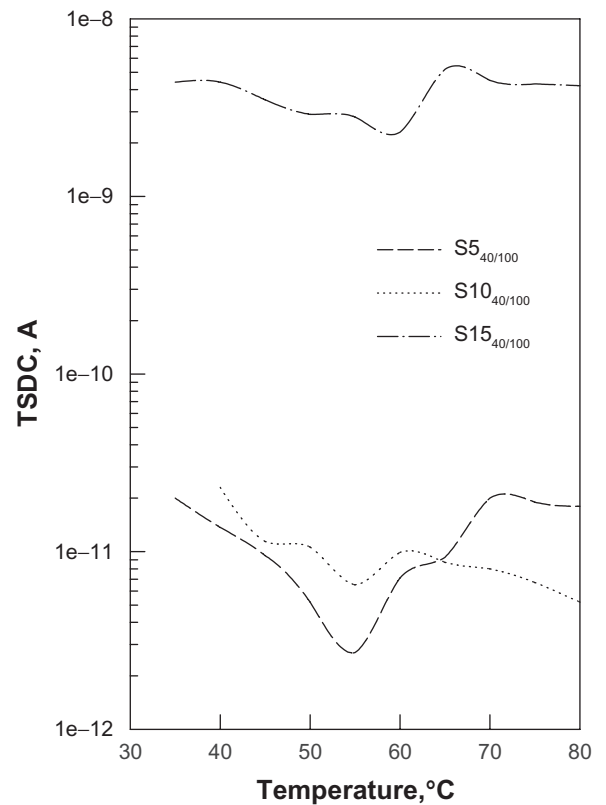
TSDC curves of PbO_2 filled CB/SBR showed a pronounced reversed peak. The spectrum consists of mainly a broad negative peak, with shoulders before and after the main peak. This negative peak caused by the release of charges introduced into the insulation matrix during lead mixing by the friction of lead particles with the polymer.[29] The peak height and peak temperature of the three samples are also listed in Table 5. The main peak is shifted to a higher T_p as MT increased. The fact that higher MT shifts the TSDC peak to higher temperatures suggests that deeper traps have been introduced. The shoulder on the low temperature side could be attributed to the relaxation of the hall system. This may be the result of the superposition of dipolar groups with a continuum distribution of relaxation times.[6] However, the shoulder on the high temperature side may be attributed to space charge.[6]

X-ray shielding ability

When gamma or X-ray radiation is incident on a finite thickness of material, the incident radiation will interact in the material and be attenuated. When a narrow

parallel beam of photon particles passes through a relatively thin shield, and if the dose point is many beam diameters away from the exit surface of the shield, we have a situation referred to in photon shielding as good geometry. This means, simply, that virtually all of the photons arriving at the dose point will be primary photons, and the dose, I, or dose rate, at a point of interest outside the shield, is related to the unshielded dose, I_0, or dose rate, at the point by[30]

$$I = I_0 \, e^{-\mu/d} \qquad (9)$$

where μ is the linear attenuation coefficient for the photons of the energy of interest in the shield material. Values of μ (cm^{-1}) for each material depend mainly on its atomic number and the energy of the incident radiation. The half thickness or the half-value layer (HVL) for a particular shielding material is the thickness required to reduce the intensity to one half its incident value, i.e. HVL is given by $\ln 2/\mu$.

μ and HVL were calculated for un-filled (S15$_{0/0}$ only for comparison) and filled composite with different MT at different operating conditions of X-ray machine (different current and applied voltage). The values of μ and HVL are given in Table 6. The linear attenuation coefficient was calculated from the plots of $\ln I/I_0$ versus the shield thickness. Figures 13–16 represent the relation of $\ln I/I_0$ versus d for all composites at 100 kV-5 mA, 100 kV-10 mA, 100 kV-15 mA and 70 kV-5 mA of X-ray machine respectively. As shown in Table 6), the un-filled SBR vulcanizates showed $\mu < \mu$ of CB filled vulcanizates $< \mu$ of samples loaded with lead oxide for those samples masticated with
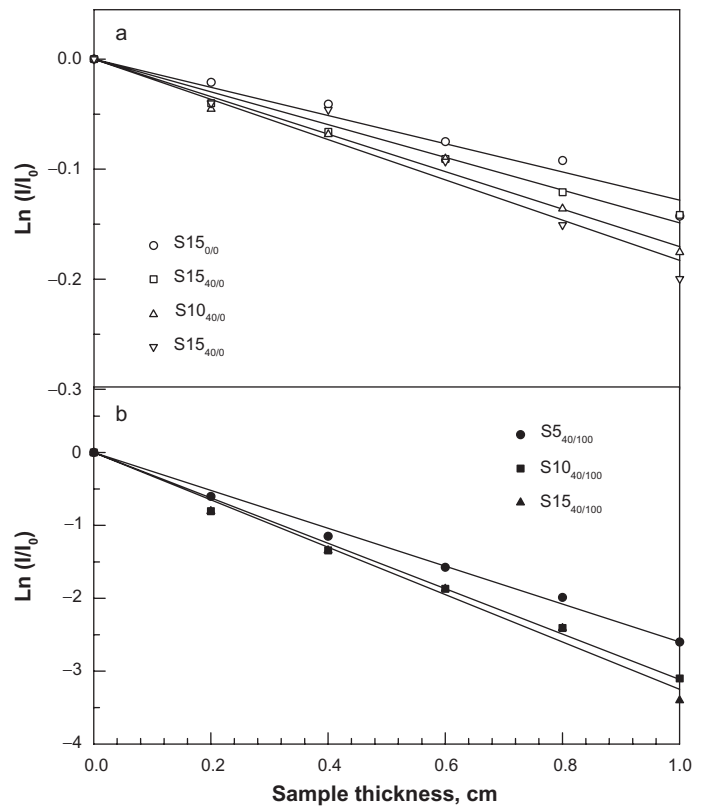

Figure 13. The dependence of $\ln (I/I_0)$ on sample thickness at 100 kV and 5 mA of X-ray machine.

the same MT. With increasing mastication time, μ appeared to increase (HVL decrease) of samples has the same filler content. This is due to the fact that there is marked increase in average cross-link density at higher MT as mentioned above.

When the applied voltage of X-ray machine rose from 70 kV to 100 kV (at the same current, 5 mA), μ decreased (HVL increased) for the same comparative samples. While, with the increasing of current

Table 6. Attenuation coefficient (μ) and half value layers (HVL) of different composites.

| Sample	100 kV–5 mA		100 kV–10 mA		100 kV–15 mA		70 kV–5 mA	
	μ (cm^{-1})	HVL (cm)	μ (cm^{-1})	HVL (cm)	μ (cm^{-1})	HVL (cm)	μ (cm^{-1})	HVL (cm)
S15$_{0/0}$	0.129	5.37	0.161	4.32	0.163	4.26	0.248	2.8
S5$_{40/0}$	0.159	4.35	0.172	4.03	0.180	3.84	0.286	2.42
S10$_{40/0}$	0.186	3.73	0.203	3.42	0.21	3.31	0.305	2.27
S15$_{40/0}$	0.189	3.66	0.222	3.13	0.212	3.27	0.341	2.03
S5$_{40/100}$	2.467	0.28	2.486	0.28	2.557	0.27	4.359	0.16
S10$_{40/100}$	2.953	0.23	2.94	0.24	3.005	0.23	5.117	0.14
S15$_{40/100}$	3.122	0.22	3.112	0.22	3.137	0.22	5.117	0.14
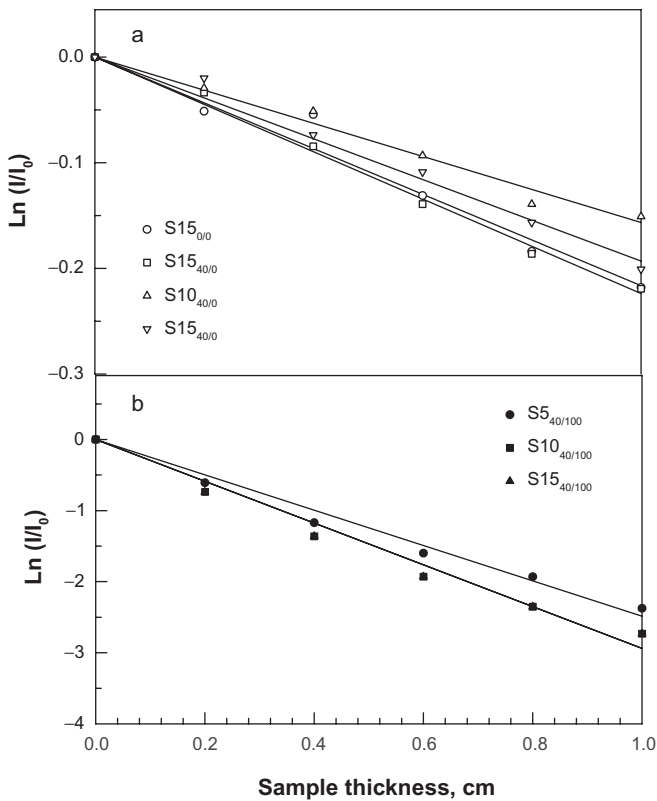
Figure 14. The dependence of ln (I/I$_0$) on sample thickness at 100 kV and 10 mA of X-ray machine.
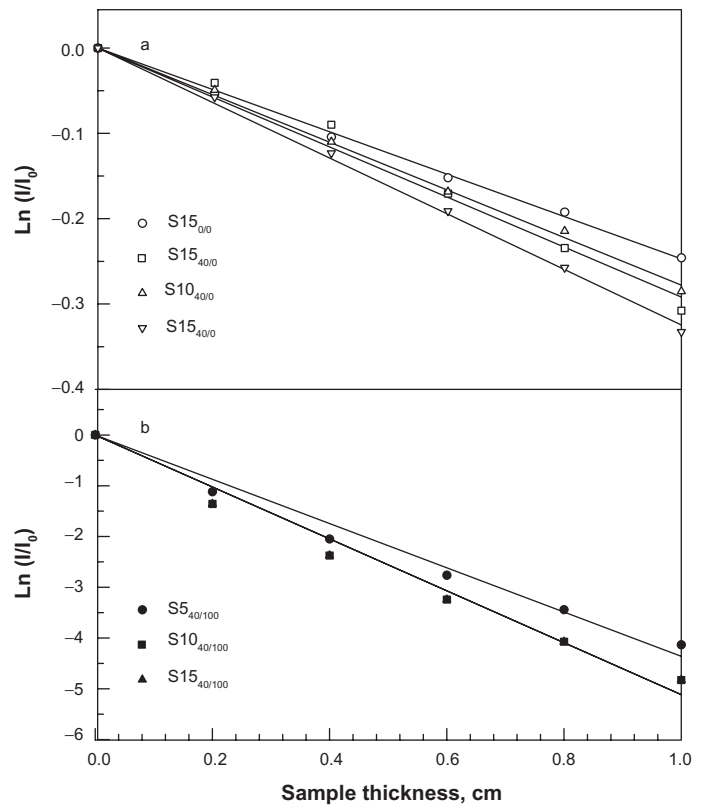

Figure 16. The dependence of ln (I/I$_0$) on sample thickness at 70 kV and 5 mA of X-ray machine.
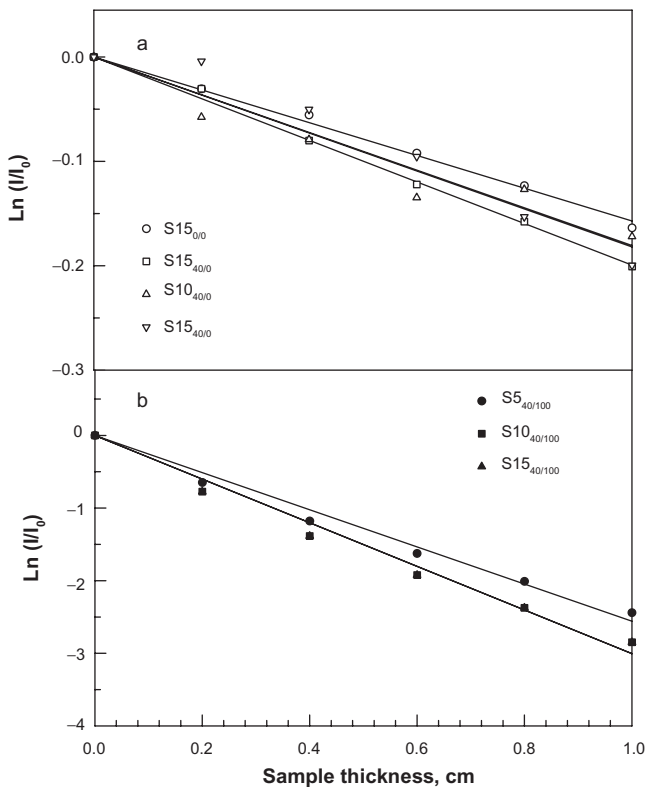

Figure 15. The dependence of ln (I/I$_0$) on sample thickness at 100 kV and 15 mA of X-ray machine.

(at constant applied voltage 100 kV), μ values are marginally changed for the same comparative samples.

As a conclusion, both μ and HVL of all composites strongly depend on: (1) the cross-linking behavior that affected by MT; (2) the type and nature of the filler used; (3) the applied voltage of X-ray machine. While they marginally affected by the current of X-ray machine. HVL of the obtained composites that loaded with lead oxide are less than 3 mm and can be used as X-ray tube housing, Equipment housings and castings, electronic devises protection, etc.

Conclusion

It may be concluded that:

1. The PbO$_2$ filled CB/SBR composites has good X-ray shielding ability and can be used in several radiation applications such as X-ray tube housing, Equipment housings and castings properties applications and electronic devises protection.

2. The higher mastication time applied for pure gum SBR before mixing increases the degree of cross-link density and enhances the electrophysical

properties of the vulcanizates and consequently enhances the network stability and filler rearrangement in rubber matrix.

3. X-ray shielding ability of PbO_2 filled conductive SBR composites is strongly dependent on filler rearrangement and distribution in the rubber matrix and the applied voltage of X-ray machine, while, it is marginally affected by the x-ray machine current.

4. The incorporation of lead oxide particles into the conductive rubber matrix creates electron traps that leads to a decrease the charge carrier mobility and hence decrease the conductivity of the obtained composite.

Disclosures

This manuscript has been read and approved by all authors. This paper is unique and is not under consideration by any other publication and has not been published elsewhere. The authors report no conflicts of interest.

References

1. Gwaily SE, Badawy MM, Hassan HH, Madani M. *Polym Compos*. 2002;23:1068.
2. Gwaily SE, Hassan HH, Madani M. *Polym Compos*. 2002;23:495.
3. Martin A, Harbison SA. "An Introduction to Radiation Protection", 3rd Ed., Chapman and Hall, London, 1986.
4. Hussain R, Ul-Haq Z, Mohammad D, Islam J. *Academ Sci*. 1997;10:81.
5. El-Sayed SM, Madani M. *Mater Manufact Proces*. 2008;23:163.
6. Madani M, Nabila A, Maziad, Rasha M, Khafagy. *J Macromol Sci (B): Physics*. 2007;46:1191.
7. Zheng H, Zhang Y, Peng Z, Zhang Y. *Polym Test*. 2004;23:217.
8. Mohanraj GT, Chaki TK, Chakraborty A, Khastgir D. *J Appl Polym Sci*. 2004;92:2179.
9. Madani M, Altaf H, Basta A. El-Sayed Abdo and Houssni El-Saied. *Progr Rubb Plast and Recycl Technol*. 2004;20:287.
10. Madani M. Polym and Polym. *Compos*. 2004;12:243.
11. Sen M, Yakar A, Guven O. *Polymer*. 1999;40:2969.
12. Madani M. *J Polym Res*. 2010;17:53.
13. Barbosa RA, Lopes RT, Tauhata L, Polenda R. *Radiat Prot Dosim*. 1999;84:353.
14. Tager A. "Physical Chemistry of Polymers", Mir Publisher, Moscow, 1978.
15. Wootthikanokkhan J, Tunjongnawin P. *Polym Test*. 2003;22:305.
16. Kumnuantipa C, Sombatsompop N. *Mater Lett*. 2003;57:3167.
17. Clough RL, Shalaby SW. Irradiation of Polymers: Fundamental and Technological Applications. *American Chewm Soci*. 1996.
18. Madani M, Badawy MM. Polym and Polym. *Composites*. 2005;13:1.
19. Kiatkamjornwong S, Pairpisit K. *J Appl Polym Sci*. 2004;92:3401.
20. Blythe AR. "Electrical Properties of Polymers", Cambridge University Press, London, New York, Melbourne, 1979.
21. Dizon ES, Hicks AE, Chirico VE. *Rubb Chem Technol*. 1974;47:231.
22. Hamed GR. *Rubb Chem Technol*. 1983;56:244.
23. Fielding-Russell GS, Rongone RL. *Rubb Chem Technol*. 1983;56:838.
24. Wan Y, Xiong C, Yu J, Wen D. *Compos Sci Technol*. 2005;65:1769.
25. Chang F, Li T. *J Matter Sci*. 2006;377:382.
26. Mattson B, Stenberg B. *Rubb Chem Technol*. 1992;65:315.
27. Bishoff MH, Dolle EF. *Carbon*. 2001;39:375.
28. Kampf G. "Characterization of Plastics by Physical Methods", Hanser Publishers, Munich Vienna, New York, 1986.
29. Motori A, Montanari GC, Gubanski S. *J Appl Polym Sci*. 1988;59:1715.
30. Chilton AB. Principles of radiation shielding, Prentice-Hall, Englewood Cliffs, NJ, 1984.